HSA
میراث جنوب غرب آسیا
HERITAGE OF SOUTHWEST ASIA

# Infrared Thermal Imaging: A Non-Destructive Technique for Pre-Screening Historical Tile's Detachment[1]

**Zohreh Chahardoli**
Department of Chemistry, Art Diagnosis Laboratory by Microchemistry and Microscopy, University of Bologna, Bologna, Italy,
https://orcid.org/0000-0003-4926-2506
zohreh.chahardoli@gmail.com

**Abstract**
Evaluating the state of conservation in historic buildings and their architectural ornament is essential to effective cultural heritage (CH) preventive preservation. Early detection of deterioration and risk factors is critical for preventing further damage and supporting informed conservation planning. Non-destructive in situ investigation methods, which allow heritage assets to be examined remotely without sampling or physical intervention, are especially valuable in this regard; among them, infrared thermal imaging (IRT) has drawn growing interest in conservation research in recent years. This study examines the effectiveness of IRT as a field technique for pre-screening the surface and subsurface features of several historical tile coverings in Golestan Palace and Soltani (Emam) Mosque buildings in Tehran. To this aim, a sequence of thermal surveys was carried out under natural environmental conditions, and the resulting thermograms were analyzed with a focus on temperature (T, °C) distribution patterns and thermal anomalies. The study's central aim was to determine IRT's capacity to pre-screen deterioration-prone areas and detect thermal irregularities linked to moisture infiltration, delamination, and structural heterogeneity within tile architectural ornaments. The findings show that IRT effectively reveals both surface and subsurface defects, offering valuable insight into the condition of architectural ornaments and building materials. Requiring neither sampling nor physical intervention, the technique supports rapid, in situ, and comparative evaluation of historic structures. These results underscore the potential of infrared thermography as an efficient complementary diagnostic tool in cultural heritage conservation and restoration, providing reliable data to inform decision-making and guide future conservation efforts.

**Keywords:** cultural heritage (CH); non-destructive testing (NDT); infrared thermography (IRT); building materials; historical tile; preventive conservation.

ACCEPTED MANUSCRIPT

## 1. Introduction

Scientific investigations of cultural heritage (CH) are of considerable importance, as they enable the gathering of valuable information (Dritsa et al., 2022; Sfarra et al., 2018), and the assessment of an artefact's preservation state constitutes a central concern of conservation science (Mercuri et al., 2011). Ensuring the long-term preservation of historic and artistic heritage increasingly depends on the development of efficient, technologically advanced tools for its analysis and monitoring (Ljungberg .1997; Meola et al., 2005). Historic façades and their architectural ornaments are continuously exposed to solar radiation, temperature fluctuations, rainfall, and wind. These stressors drive cyclic thermal and moisture-related changes that, over time, produce fissuring, water

[1] The Persian version of this paper, under the following title, is also published in this issue of HSA:
**تصویربرداری حرارتی فروسرخ: روشی غیرتخریبی برای ارزیابی وضعیت حفاظتی کاشی‌های تاریخی پیش از مداخله مرمتی**

infiltration, loss of adhesion, and the detachment of ceramic elements (de Melo et al., 2024). Because such processes often begin below the visible surface, non-destructive techniques that can detect them early have become central to conservation practice (Bashevskaya et al., 2017). They provide diagnostic data for pre-intervention assessment and reduce the risk of poorly targeted repairs (Dritsa et al., 2022; Barbosa et al., 2021).

Infrared thermography (IRT) is particularly well suited to this role. It maps surface and subsurface temperature remotely and without contact, acquires two-dimensional data rapidly and at high resolution, and is portable enough for in situ survey (Costanzo et al., 2015; Meola et al., 2005; Vavilov et al., 1997). Recent instrumental developments have also made thermal cameras considerably more affordable (Gade & Moeslund, 2014). IRT can be applied in active mode, where controlled thermal stimulation reveals subsurface discontinuities such as voids, delaminations, and inclusions (Bashevskaya et al., 2017; Mercuri et al., 2011), or in passive mode (PT), which relies on naturally occurring thermal gradients such as diurnal solar heating and cooling. Passive operation is especially relevant to large architectural surfaces, where artificial stimulation is impractical(Figure-1).

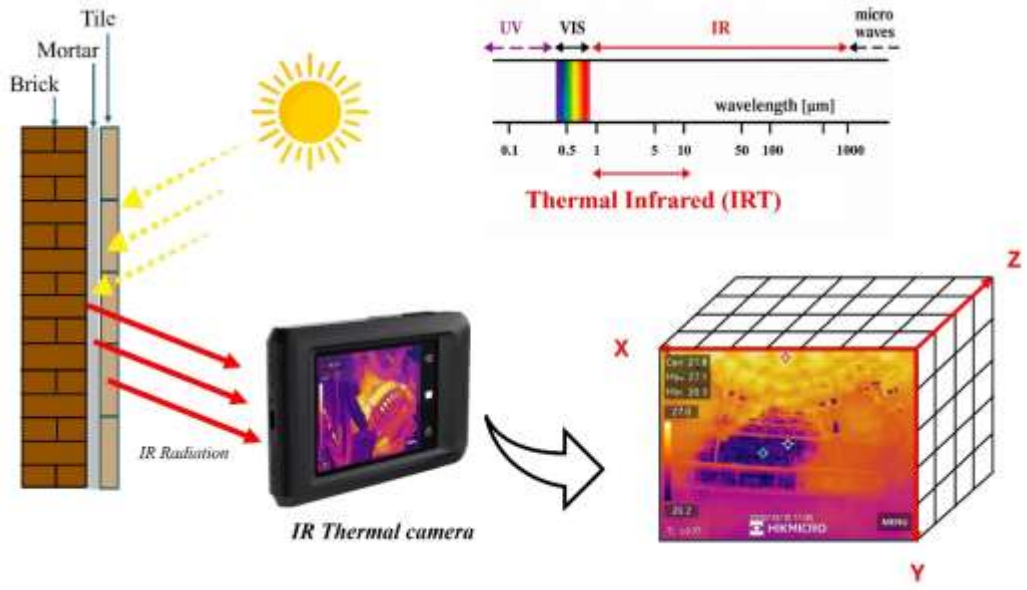



Figure. 1 Overview of the IRT workflow for pre-screening tile detachment in historic buildings.

Within cultural heritage, IRT applications fall into several established lines of research. The first is moisture detection in building envelopes, which has a long history (Bomberg & Shirtliffe, 1978). Damp zones typically appear as cooler regions because of evaporative cooling and higher thermal inertia, and wall surface temperature combined with ambient relative humidity allows condensation risk to be evaluated through the dew point (Grinzato et al., 2002). The second is the inspection of masonry and wall paintings, where IRT has been used to locate detachments, voids, and hidden structures in frescoes and murals (Tortora et al., 2016). The third concerns tessellated and ceramic surfaces. Here, passive and active thermography have been applied to mosaic pavements and structures (Theodorakeas et al., 2015; Theodorakeas et al., 2018; Ftikou, 2016; Moropoulou et al., 2000), and the detachment of modern adhered ceramic cladding has been linked to cyclic hygrothermal loading (de Melo et al., 2024). Beyond architecture, PT has also been applied to

ACCEPTED MANUSCRIPT

movable heritage such as ancient books (Paoloni et al., 2020; Orazi, 2020; Mercuri et al., 2018; Sfarra et al., 2018a; Sfarra et al., 2018b; Tortora et al., 2019) and bronze artefacts (Yang et al., 2022), although these contexts differ substantially from layered façade systems.

These studies leave a specific gap. Historic glazed tilework is a multilayer system composed of a thin vitreous glaze, a ceramic body, a bedding mortar, and a brick or stone substrate. Its thermal behaviour relative to adjacent materials has received little direct attention. The layers differ in thermal expansion coefficient, volumetric heat capacity, and thermal conductivity, so each heating and cooling cycle generates thermal gradients and stresses at their interfaces. These stresses are most critical in the brittle glaze layer and at the tile–mortar bond, and they may lead to microcracking, glaze spalling, and eventually detachment of the glaze from the body or of the tile from the substrate (Fitzner et al., 2002; Hall & Hoff, 2011). Moisture ingress further amplifies this pathway through freeze–thaw action and salt crystallisation. Because detachment initiates at hidden interfaces, it is rarely detectable by visual inspection alone. A second difficulty in practice is distinguishing active deterioration from past restorations, such as replacement tiles, modern mortars, and infills, which may look similar to the eye but differ in material and therefore in thermal response.

These challenges are especially pronounced in Qajar-period architecture (1789–1925 AD). Qajar tilework moved away from the geometric abstraction of earlier Islamic periods towards pictorial narrative, rich polychrome palettes, and European artistic influence. The crowning achievement of Qajar tilework is preserved at the UNESCO World Heritage-listed Golestan Palace in Tehran, whose walls are covered in spectacular tile murals depicting subjects ranging from majestic battle scenes to delicate repeating floral motifs (UNESCO, 2013; Zandieh et al. 2013). Qajar decorative schemes combine glazed tile, brick, stone, and mortar within single compositions and have frequently been repaired over time. This material heterogeneity makes them both highly susceptible to interfacial thermal stress and moisture-related decay and difficult to assess by conventional visual survey.

This study therefore evaluates whether a handheld thermal camera (HIKMICRO Pocket Series), operated in passive mode, can serve as a rapid in situ pre-screening tool for Qajar tiled façades and their associated brick, stone, and masonry ornaments. The first aim is to establish whether glazed tile surfaces respond to natural solar loading differently from the adjacent brick, stone, and mortar, and whether thermal anomalies concentrate at the interfaces between these materials. Building on this, the study examines whether such a portable instrument can distinguish anomalies arising from moisture ingress from those consistent with tile detachment, and from the signatures of past restoration interventions. Finally, it considers whether these thermal signatures can be translated into a practical basis for prioritising restoration interventions according to anomaly type.

The study rests on the expectations grounded in the thermophysical behaviour of layered façade systems. First, detached or delaminated tiles are to show a localised thermal contrast relative to well-bonded areas of the same material, because the air gap behind them acts as an insulating layer. Moisture-affected zones are expected to remain persistently cooler than sound areas and to show a reduced diurnal temperature amplitude, due to evaporative cooling and increased thermal inertia. Restored areas, such as modern mortars replaced instead of tiles, are expected to produce thermal signatures that differ from the original tiles.

## 2. Materials and Methods

### *2.1. Buildings under investigation*

ACCEPTED MANUSCRIPT

To illustrate the range of applications of IRT in CH for tilework conservation, two historic buildings constructed with diverse materials were selected as case studies. We analyzed the Soltani (Emam) Mosque and Golestan Palace, a UNESCO World Heritage Site (Figure 2), both located in Tehran and dating to the Qajar dynasty (19th century), under the supervision of the Ministry of Cultural Heritage, as listed in Table 1.

**Table 1.** Overview of historic buildings selected as case studies for infrared thermography (IRT) analysis

| *Building Names* | *No.* | *Construction Period* | *Architectural Material(s)* | *Place* |
|---|---|---|---|---|
| ***Soltani Mosque*** | SM1 | Qajar Dynasty (19th Century) | Tilework; Brickwork; | Tehran |
| | SM2 | Qajar Dynasty (19th Century) | Tilework; Brickwork; | Tehran |
| ***Golestan Palace*** | GP1 | Qajar Dynasty (19th Century) | Tilework; Brickwork; Stucco; Stone; | Tehran |
| | GP2 | Qajar Dynasty (19th Century) | Tilework; Brickwork; | Tehran |
| | GP3 | Qajar Dynasty (19th Century) | Tilework; Brickwork; | Tehran |
| | GP4 | Qajar Dynasty (19th Century) | Tilework; Stucco; Stone; | Tehran |

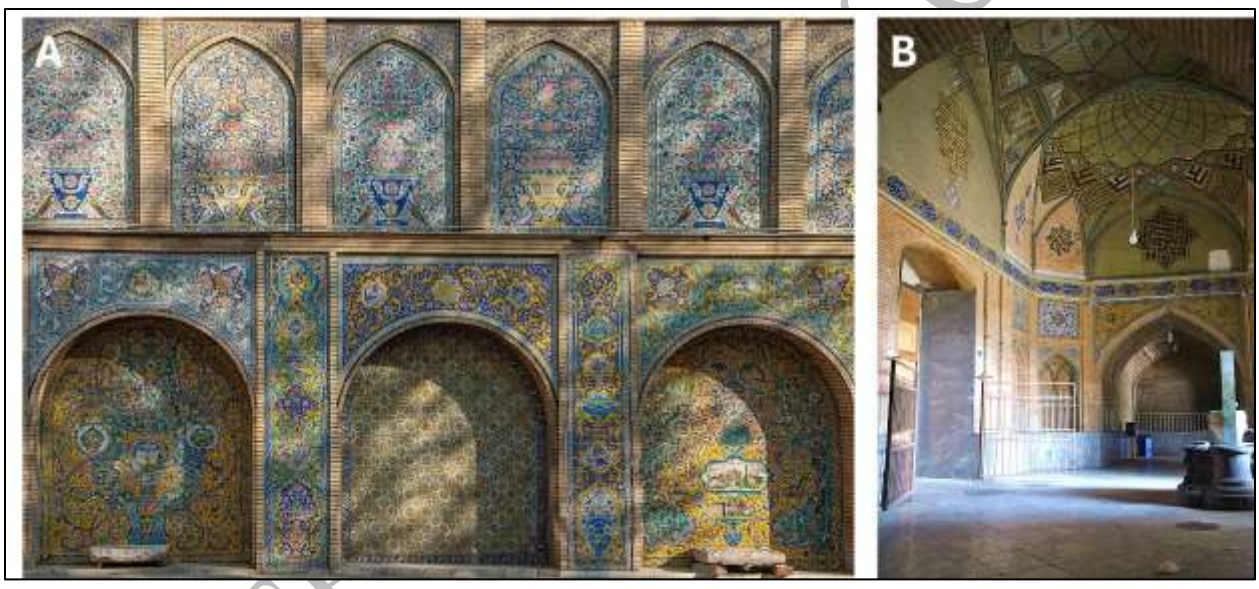



Figure 2. Interior space of the two historical buildings (HBs) investigated in this study: (a) Golestan Palace (Allardice, 2012) , (b) Soltani (Emam) Mosque; Tehran.

### *2.2. Infrared Thermal Imaging (IRT)*

Thermal inspections were carried out using a HIKMICRO Pocket Series infrared thermal camera, equipped with a high-resolution VOx detector, an 8-megapixel optical camera, and a 3.5-inch LCD touchscreen. The device offers a thermal resolution of 256 × 192 pixels (49,152 pixels) and a thermal sensitivity of <40 mK at 25°C (NETD). Its measurement range spans −20°C to 400°C, with an accuracy of ±2°C or ±2% of the reading, whichever is greater. A frame rate of 25 Hz enables rapid thermal inspection, while multiple imaging modes—including thermal, fusion, picture-in-picture (PIP), and optical—combined with the integrated 8-megapixel optical camera, offer enhanced flexibility for image interpretation and data analysis.

ACCEPTED MANUSCRIPT

Ambient temperature (28 ± 2 °C) and relative humidity (23–27%) were recorded at 2 m from the façade at each acquisition. Images were taken in passive mode (PT), at a camera-to-object distance of 1.5 to 4.5 m. At this distance the footprint of a single pixel on the surface is approximately 5 mm to 20 mm, which sets the smallest feature that can be resolved. To limit reflections from the glazed surfaces, the camera was kept as close to normal incidence as site access allowed, with viewing angles not exceeding 45° from the surface normal. Each area was also imaged from at least two angles so that reflections could be identified.

The compact, lightweight, and portable design of the HIKMICRO Pocket Series allows for straightforward operation in field conditions. A key advantage of this technique lies in its capacity to perform direct, non-contact thermal imaging of historic and artistic objects without requiring surface preparation or physical intervention.

### *2.3. Image Processing and Data Analysis*

Thermal images were exported in JPEG format and analysis were processed in HIKMICRO Analyzer (v1.0.2 build240924), to locate candidate anomalies. To facilitate the interpretation of thermal data, several image-processing and visualization techniques were applied. Data fusion algorithms were employed to enhance the visualization of thermal variations and orientation, while different color palettes were used to improve temperature classification and anomaly detection. The White Hot and Black Hot grayscale palettes were applied to emphasize structural details, the Rainbow palette enhanced contrast for subtle temperature differences, and specialized palettes such as Ironbow and Lava provided intuitive visualization of thermal patterns, with warmer areas represented by brighter or warm tones and cooler areas by darker or blue tones. Thermographic data were analysed at two levels: qualitative interpretation of thermal patterns and quantitative analysis of temperature values.

*Qualitative interpretation.* Thermograms were examined to locate candidate anomalies, such as areas warmer or cooler than their surroundings, patterns crossing material boundaries, and regular geometric outlines. Colour palettes were used for visualisation only, with a fixed temperature span within each acquisition series.

*Quantitative analysis.* Temperatures were corrected as single point or ROI (min & max temperature) for material-specific emissivity and reflected apparent temperature.

Images displayed in the figures use the linear colour scale. A fixed temperature span was kept within each acquisition series so that images could be compared over time. Visible–thermal fusion images were used for orientation and quantitative analysis.

Figure 3 presents the spatial temperature distribution of the investigated area in both 2D and 3D. In the 2D (X–Y) view, the color distribution reveals considerable thermal heterogeneity, with recorded temperatures ranging from approximately 19.3°C to 26.1°C. The 3D representation maps these values onto the Z-axis, with warmer regions appearing as elevated surfaces and cooler areas as depressions, offering a more intuitive view of the thermal gradients. A distinct central zone with lower temperatures than its surroundings suggest the influence of environmental or structural factors, while more pronounced fluctuations near the edges may reflect boundary effects or sampling limitations.

ACCEPTED MANUSCRIPT

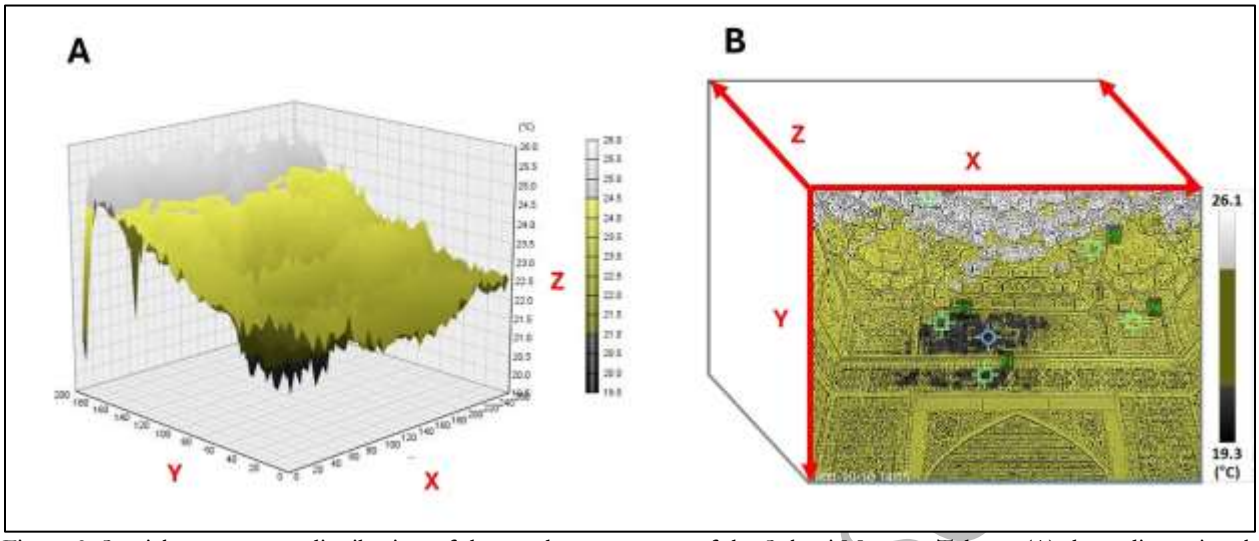



Figure 3. Spatial temperature distribution of the southern entrance of the Soltani Mosque, Tehran: (A) three-dimensional representation of the thermal surface, with temperature plotted along the Z-axis; (B) two-dimensional thermal map in the X–Y plane, showing a adjusted temperature range of 19.3–26.1°C

The combined use of 2D and 3D thermal maps provides a comprehensive visualization of the spatial temperature distribution, facilitating the identification of critical areas, thermal anomalies, non-uniform temperature patterns, and regions characterized by high thermal gradients.

## 3. Results and Discussion

To monitor anomalies, the indoor and outdoor glazed tiles of Golestan Palace and the Soltani Mosque were investigated using an infrared thermal camera, with different areas assessed according to their materials and condition. All data acquisition was conducted under mild weather conditions. Based on the type of masonry and ornament used in each building, the resulting database was categorized into two groups.

Thermal inspections were conducted in passive mode, relying on naturally occurring thermal gradients. Active thermography was not used because the aim was a rapid, in situ preliminary screening of large, fragile heritage surfaces open to the public. Anomalies were interpreted as relative thermal contrasts rather than absolute temperatures. Suspected delaminations and moisture-affected areas therefore require confirmation by complementary non-destructive techniques.

### *3.1. Golestan Palace (GP) Database*

***GP1:*** To assess the state of conservation and delamination of the glazed tiles, based on the thermal image data (Figure. 4 & 5, Table 2), various parts and materials were analyzed through region- and single-point analysis. Figure 4A shows the thermogram of the GP1 site. Surface temperatures ranged from 24.0 °C to 36.9 °C. Within the sheltered space, temperatures ranged from 24 °C to 27 °C, with the minimum (P3: 24.1 °C) recorded on the wooden door at the back of the room. Temperatures increased progressively towards the exposed outer areas. The highest values were recorded on the stone surfaces at the base of the structure (P2: 35.0 °C; P1: 36.8 °C) and on the stairs (R2: 30.0–35.8 °C), glazed tile surfacesis detailed in Figure 5 and Table 2.

Several factors may contribute to these differences. The most evident is solar exposure. The sheltered space received no direct radiation at the time of acquisition, whereas the façade, stone base

ACCEPTED MANUSCRIPT

and stairs were directly sunlit. More precisely, they also received a high irradiance at that time of day. The low temperatures in the sheltered space, including at the wooden door, are therefore primarily attributable to shading. Because the wood and stone surfaces were not under comparable exposure, these data do not allow the effect of material properties to be isolated. Although direct solar radiation can temporarily raise the surface temperature of wood, its low heat storage capacity causes absorbed heat to dissipate quickly, resulting in lower thermal stability (Steinhagen & Haslett, 1993).
Material properties may nonetheless modulate the response. These differences arise from their physical properties, including specific heat capacity, density, and thermal conductivity, which collectively determine the volumetric heat capacity and, ultimately, the thermal inertia of each material (Incropera et al., 2011; Çengel & Ghajar, 2015).

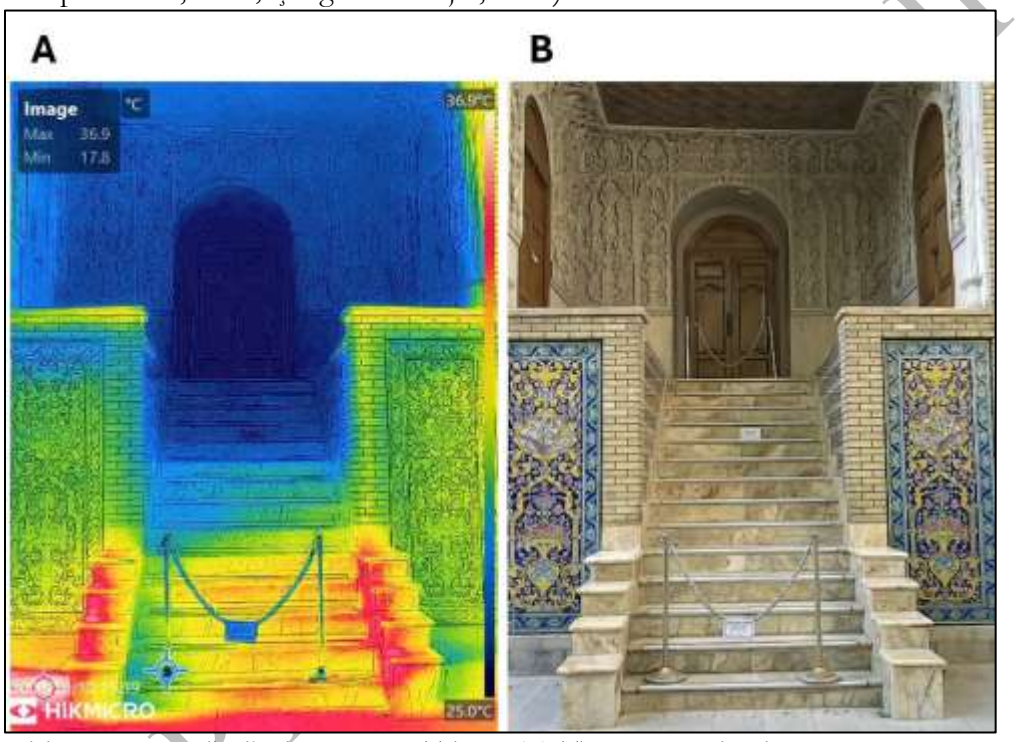



Figure 4. Spatial temperature distribution at GP1, Tehran. (A) Thermogram showing a temperature range of 24.0–36.9°C; (B) visible-light image of GP1.

The highest temperatures, as Figure. 5 shown, were associated with the stone surfaces at the base of the structure, with points P2 and P3 (35.0°C and 36.8°C, respectively) identified as the warmest areas. The stairs at R2 similarly represent one of the warmest regions in the structure, with a temperature range of 30.0–35.8°C. Due to their high density and high volumetric heat capacity, stones can absorb a greater amount of thermal energy under identical radiation conditions (Incropera et al., 2011). This characteristic allows stone surfaces not only to absorb more heat but also to store and release it over a longer period, a phenomenon known as high thermal inertia, and one of the primary factors contributing to stone's higher surface temperature relative to other materials (Hall & Hoff, 2011). Heat transfer in these materials occurs mainly through conduction: the higher thermal conductivity of stone, compared with wood and other porous materials, results in greater heat flux into the material and more rapid distribution of thermal energy throughout its

ACCEPTED

volume (Çengel & Ghajar, 2015; Neville, 2012). Consequently, once heated, stone cools more slowly than lightweight materials. The details of the data acquisition conditions are summarized in Table 2.

Table 2. GP1 site, IRT region and point analysis

| ***Measurements*** | ***Temp.*** | ***Measurements*** | ***Temp.*** |
|---|---|---|---|
| *Image: Max. Temp.* | 36.9°C | *R1: Max. Temp.* | 32.6°C |
| *Image: Min. Temp.* | 24.0°C | *R1: Min. Temp.* | 28.3°C |
| *P1* | 36.8°C | *R2: Max. Temp.* | 35.8°C |
| *P2* | 35.0°C | *R2: Min. Temp.* | 30.0°C |
| *P3* | 24.1°C | *R3: Max. Temp.* | 31.7°C |
| *P4* | 26.7°C | *R3: Min. Temp.* | 29.1°C |

The glazed tiles in the two frames on the left and right sides of the stairs (R1 and R3) demonstrate an intermediate thermal response. Temperature differences are greater in R1 than in R3, as heat transfer from the stone is visible in the lower part of R1. The upper part of both frames has a lower temperature, which may suggest a different state of conservation, although no clear tile detachments are reported.

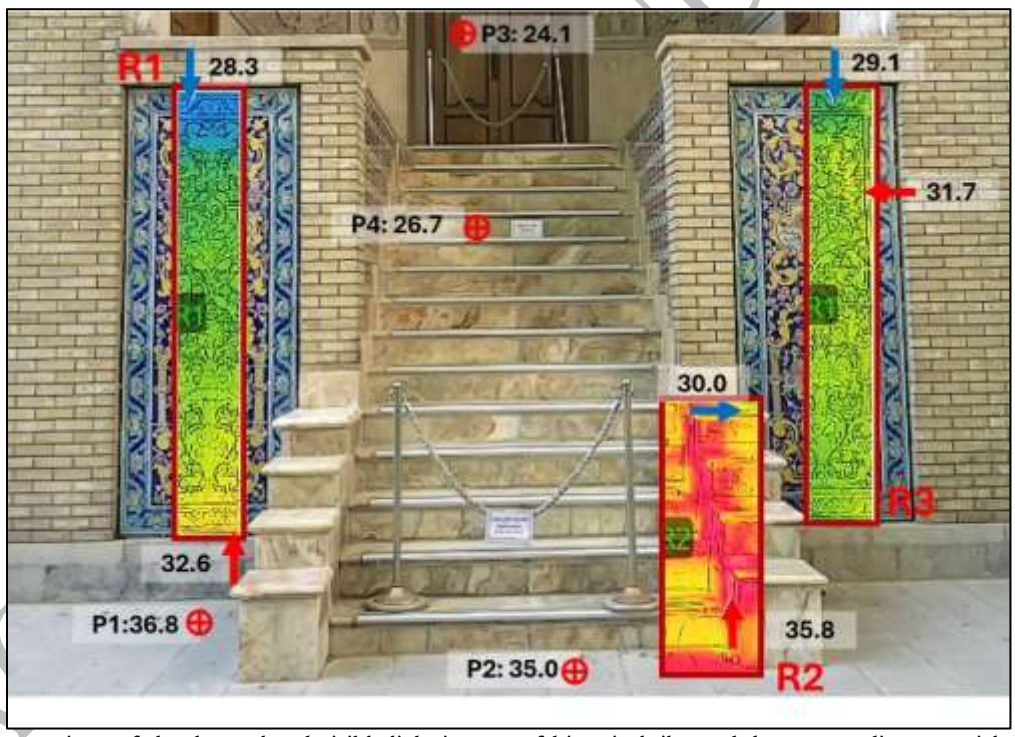



Figure 5. Comparison of the thermal and visible light images of historical tiles and the surrounding materials at GP1.

***GP2:*** The results for the middle column frame show an anomaly, with spots of temperature variation. The mean temperature value for the GP2 frame is approximately 32.5°C, accounting for the effects of light and shadow (Figure 6). The glazed tiles located in R1, the central upper part of the image, exhibit lower temperatures compared to the other areas. Measurement points P1 and P2 recorded greater temperature variation than the other areas, indicating lower heat absorption and

ACCEPTED MANUSCRIPT

retention at these surfaces, as shown in Figure 6c. This behavior can be attributed to material differences, specifically the use of gypsum for the reinforcement and restoration of the glazed tiles. The glassy glaze layer, due to its lower porosity and dense surface structure than brick, has a greater capacity to absorb radiant energy while exhibiting slower thermal exchange with the surrounding environment. The mortar joints between the bricks may also contribute to the moderation of surface temperature, owing to their heterogeneous structure and higher moisture absorption capacity (Incropera et al., 2011; Çengel & Ghajar, 2015). The higher porosity of these materials reduces their effective density and, consequently, their thermal energy storage capacity (Lawrence & Walker, 2006).

In contrast, the bricks surrounding the frame also show lower temperatures than the glazed tiles, with point P3 (approximately 27°C) identified as the coolest region. This behavior, as noted above, can be attributed to the higher porosity of brick and the presence of a capillary network within its structure, which enhances heat exchange with the surrounding air and reduces the thermal stability of the surface (Lawrence & Walker, 2006).

***GP3:*** The thermal image shows an arched, richly tiled decorative panel (likely a mihrab-style niche). The color scale ranges from blue (coolest) through green and yellow to red and pink (warmest), with a recorded maximum of 32.2°C and minimum of 24.7°C. The arch framing the panel and its outer border appear predominantly red/orange, indicating the warmest surface temperatures, as shown in Figure 7.

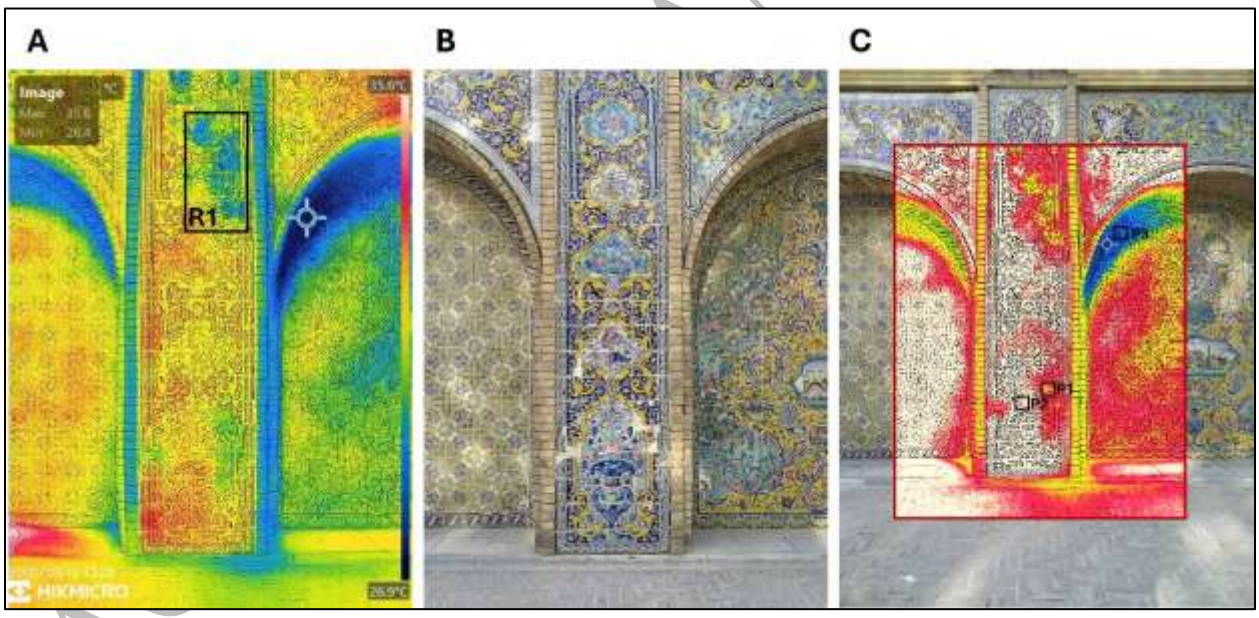



Figure 6. GP2 illustrates the surface temperature distribution of tiled panel and its surrounding materials (A) based on the thermal image and (B) the corresponding visible light image. (C) the combination of visible and IR light image enables simultaneous analysis of thermal behavior and surface material characteristics. The recorded temperature range in the thermal image is approximately 26.9 to 35.6°C, indicating significant thermal heterogeneity across the investigated surface.

The upper-central portion of the niche, including the arch's inner curve and the area just below it, appears blue and green, noticeably cooler than the surrounding ornamental surface. The lower temperatures observed beneath the arch may be attributed to the shading effect of the arch's overhang, which limits direct solar radiation reaching this recessed area and exposes it primarily to

ACCEPTED MANUSCRIPT

indirect light for much of the day, compared with the more exposed surrounding surfaces. Sheltered spaces such as this often experience different, and often more stable, airflow patterns than exposed surfaces, which can further moderate surface temperature, as similarly observed at GP1. Localized moisture content or differences in material composition in this area also cannot be excluded as contributing factors, consistent with the moisture-related thermal anomalies discussed in introduction. The main decorated field within the niche, comprising the bulk of the carved and inscribed area, appears yellow, indicating intermediate-to-warm temperatures fairly uniform across most of the panel, with a small reddish-orange patch near the lower-center suggesting a locally warmer spot.

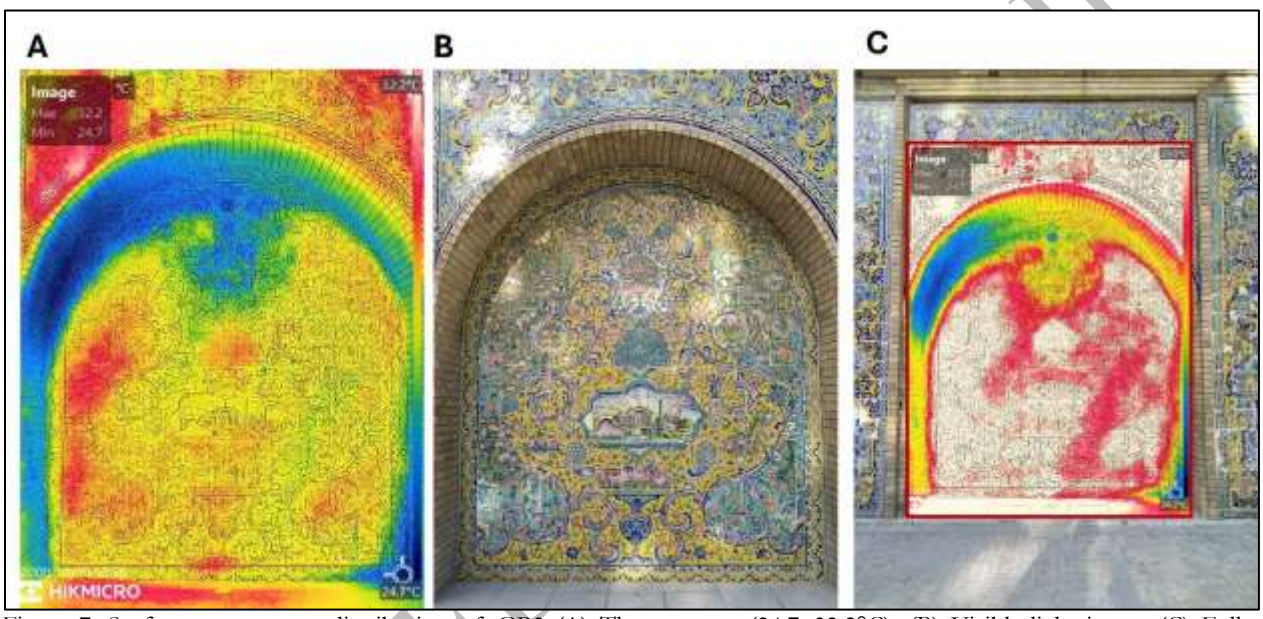



Figure 7. Surface temperature distribution of GP3 (A) Thermogram (24.7–32.2°C). (B) Visible-light image (C) Full-context photograph with inset thermogram location indicated (red box)

***GP4:*** Figure 8 illustrates GP4 21.5°C (min) to 31.0°C (max), a deep, recessed archway, where the interior surfaces of the alcove—including the back wall, side walls, and floor—display markedly lower temperatures (predominantly in the 21.5–24°C range) than the surrounding, directly exposed surfaces. The tile-decorated archivolt framing the arch exhibits intermediate temperatures, while the exterior surfaces at the top and bottom of the frame, which receive direct solar radiation, reach the higher values, and the highest recorded values belongs to stone ground (up to 31.0°C). This pronounced thermal contrast provides clear visual confirmation of the shading effect discussed previously: the deep architectural recession of the alcove substantially limits direct solar exposure to its interior surfaces, resulting in a distinct and well-bounded cooler zone relative to the more exposed surrounding architecture.

with a different color palette (the "iron/rainbow" scale, white–yellow–orange–red)

Figure 8c presents the GP4 with six measurement points (P1–P6) distributed across the interior and surrounding surfaces, recorded under the low temperature range (21.5–26.5°C) in order to see a better detail of anomalies. The lowest values were recorded at P3 (22.8°C) could indicate to damp and poor air circulation and P5 (24.2°C), both located within the shaded interior of the alcove,

ACCEPTED MANUSCRIPT

consistent with the reduced solar exposure discussed previously. P1 and P2, positioned nearer the arch's inner curve, recorded intermediate temperatures (25.8°C and 27.1°C, respectively), reflecting a transitional zone between the shaded recess and the more exposed archivolt. The highest reading, at P6 (29.4°C), was recorded on the exterior stone surface at the ground, directly exposed to solar radiation, as we discussed the stone thermal characteristics. These point measurements corroborate the broader thermal pattern observed across the frame, confirming a consistent gradient from the cooler, shaded interior toward the warmer, sun-exposed exterior surfaces.

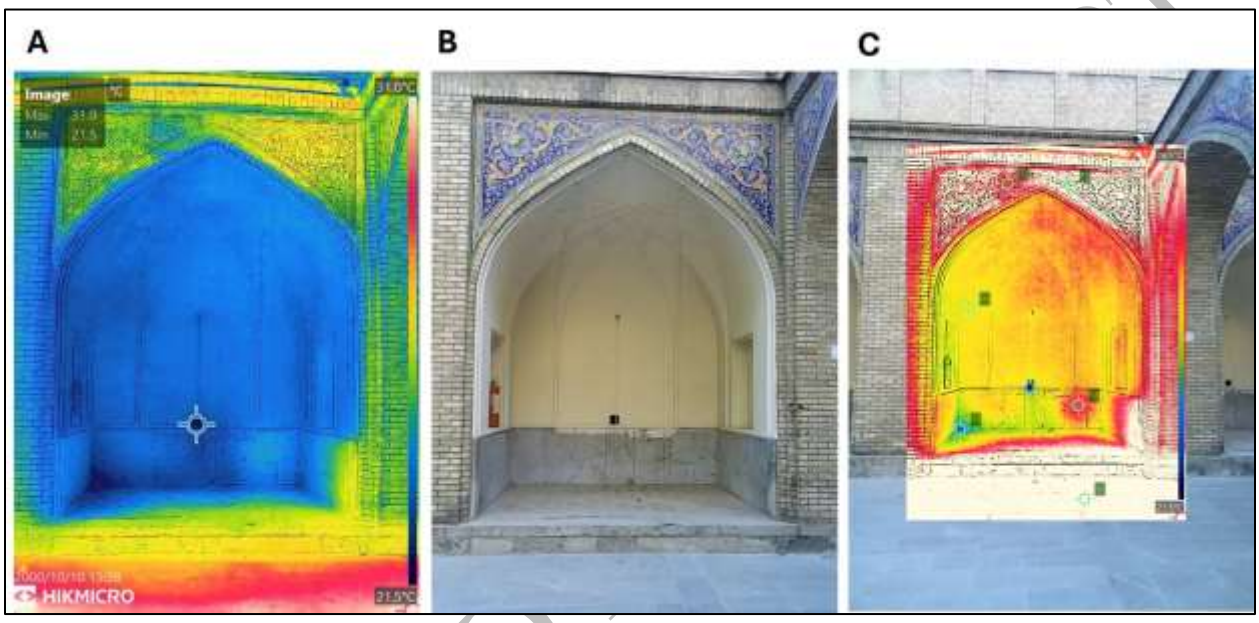



Figure 8. . (A) Thermogram (21.5–31.0°C) (B) Visible-light (C) Visible-light image with inset edge-enhanced thermogram (21.5–26.5°C) showing a warm structure (red/orange), intermediate tiled band (yellow-green), and a cooler anomalous zone (blue).

### *3.2. Soltani Mosque (SM) Database*

***SM1:*** Figure 9 presents a comparison of the visible-light image with the thermal distribution, of IRT images of the tiled surface of the *muqarnas,* a three-dimensional architectural ornament, on the southern entrance of the Soltani Mosque in Tehran, together with the selected measurement points. The visible-light image clearly illustrates the geometric and decorative details of the *muqarnas* and inscriptions and serves as the reference image for the alignment and interpretation of the thermal data. As shown in Figure 9b, no visible irregularities or indications of deterioration or structural damage can be identified in the *muqarnas* or the inscriptions under visible light imaging.

In contrast, the infrared thermal image and the temperature distribution map reveal significant thermal variations in the same regions that are not discernible in the visible-light image. The infrared thermogram shows a heterogeneous temperature distribution across the tiled surface of the *muqarnas*. The central and lower portions of the image exhibit lower temperatures than the upper areas, a difference that is clearly reflected in the color scale. The designated with four measurement points (P1-P4) display noticeable temperature differencesAs shown in Figure 9a, the ROI containing point P1 was 3 °C cooler than the reference area at P2, although both were located at the same height and under similar environmental conditions. This localised anomaly suggests a specific cause,

ACCEPTED

such as moisture infiltration, a subsurface void, or a material or construction difference that may lead to tile detachment. Further investigation is required to confirm its origin.

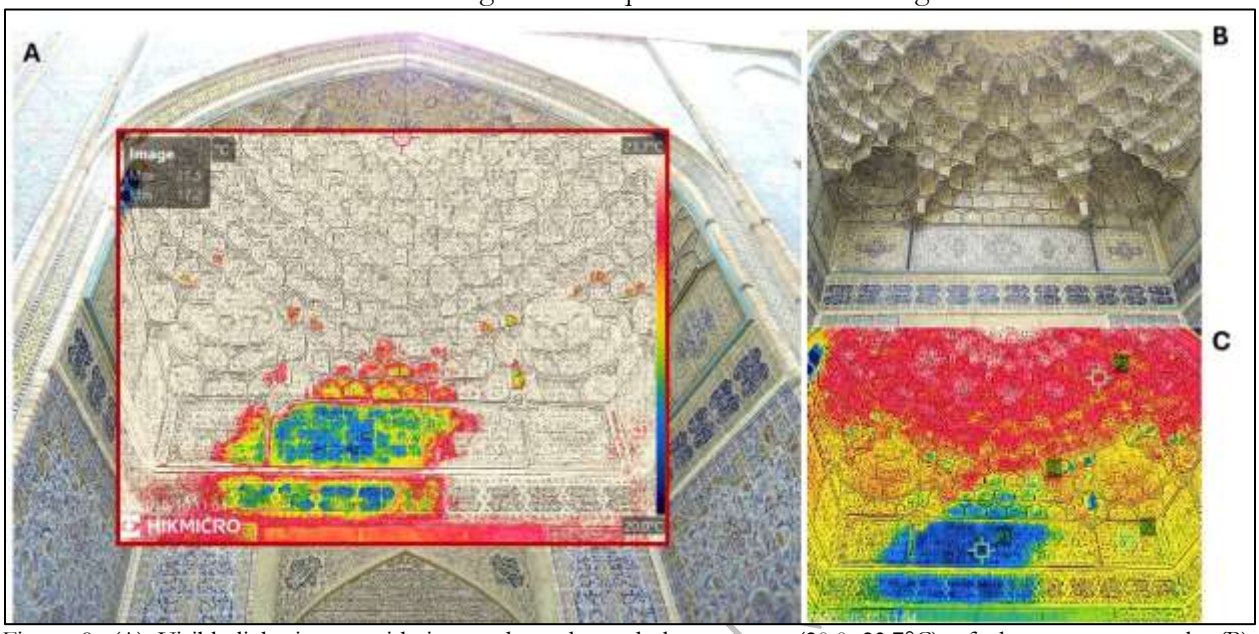



Figure 9. (A) Visible-light image with inset edge-enhanced thermogram (20.0–23.7°C) of the muqarnas vault. (B) Visible-light close-up of the muqarnas and tiled band. (C) Thermogram (17.2–27.5°C) showing a warm muqarnas structure (red/orange), intermediate tiled band (yellow-green), and a cooler anomalous zone (blue).

P3, located within the upper muqarnas structure, recorded the highest temperature, consistent with its greater solar exposure and complex three-dimensional geometry. P4, positioned at the transition between the muqarnas and the tiled band below, recorded an intermediate value, reflecting the gradual thermal transition between these two architectural elements. Within the tiled band, P2 recorded a moderate temperature consistent with the surrounding surface.

Table 3. IRT Max, min, and point-specific T (°C) analysis, recorded at GP4, SM1 and SM2 sites.

| ***GP4 Measurements*** | ***Temp.*** | ***SM1 Measurements*** | ***Temp.*** | ***SM2 Measurements*** | ***Temp.*** |
|---|---|---|---|---|---|
| *GP4-Image: Max. Temp.* | 31.0°C | *SM1-Image: Max. Temp.* | 27.5°C | *SM2-Image: Max. Temp.* | 29.2°C |
| *GP4-Image: Min. Temp.* | 21.5°C | *SM1-Image: Min. Temp.* | 17.2°C | *SM2-Image: Min. Temp.* | 22.2°C |
| *GP4-P1* | 25.8°C | *SM1-P1* | 20.9°C | *SM2-P1* | 24.5°C |
| *GP4-P2* | 27.1°C | *SM1-P2* | 23.6°C | *SM2-P2* | 25.9°C |
| *GP4-P3* | 22.8°C | *SM1-P3* | 25.8°C | *SM2-P3* | 26.0°C |
| *GP4-P4* | 25.5°C | *SM1-P4* | 23.1°C | *SM2-P4* | 25.2°C |
| *GP4-P5* | 24.2°C | | | *SM2-P5* | 28.3°C |
| *GP4-P6* | 29.4°C | | | | |

***SM2:*** The IRT and single-point analysis results obtained from SM2 reveal the thermal distribution pattern of the southern *ivan* of the Soltani Mosque in Tehran (Table 3). Figure 10b recorded temperature range spans 22.2–29.1°C, as Figure 10a more focused on lower range of temperature, in order to obtain detailed variation in lower rangs of temperatures. The majority of the vaulted surface displays relatively uniform, moderate temperatures, while a distinct warmer band is visible along the base of the structure, likely corresponding to a transition toward an adjacent wall or lower

ACCEPTED MAN

architectural element. The highest recorded value, at P5 (28.3°C), corresponds to a patterned tile motif in the upper section of the frame, suggesting a locally warmer surface possibly attributable to differences in material or surface exposure. Points P2 and P3, located along the base of the arch, recorded intermediate and comparatively consistent temperatures (25.9–26.0°C), reflecting relatively homogeneous thermal behavior across this section of the ornament, except P1and P4 indicate the blue and yellow reigns (24.5–25.2°C), suggest a careful investigation. Part of this thermal heterogeneity can be attributed to the presence of a perforated brick window and the increased air circulation in this area. At the same time, another portion of the observed temperature variations may result from inconsistencies in the adhesion of tile layers to the structural substrate and differences in the thermal behavior of the underlying materials.

Based on the acquired thermograms, air circulation and heat transfer toward the higher regions of the *ivan* can be observed in this historic structure. As shown in Figure 10b, the warmest areas of the *ivan* correspond to the sections of *mosaic tilework* containing the *Kufic* inscription and the apex of the arch located at its highest point, where the maximum recorded temperature reaches approximately 28.3°C (P5, Figure 10a). This concentration of heat in the upper areas of the arch can be attributed to differences in material composition, the thickness of material layers, and the capacity of the mosaic tiles to absorb and retain thermal energy. In addition, the observed pattern indicates the influence of convective air movement on heat accumulation in the upper parts of the *ivan*. This phenomenon, together with environmental conditions, may affect the thermal behavior of the structure and, in the long term, influence the conservation condition of its architectural ornaments.

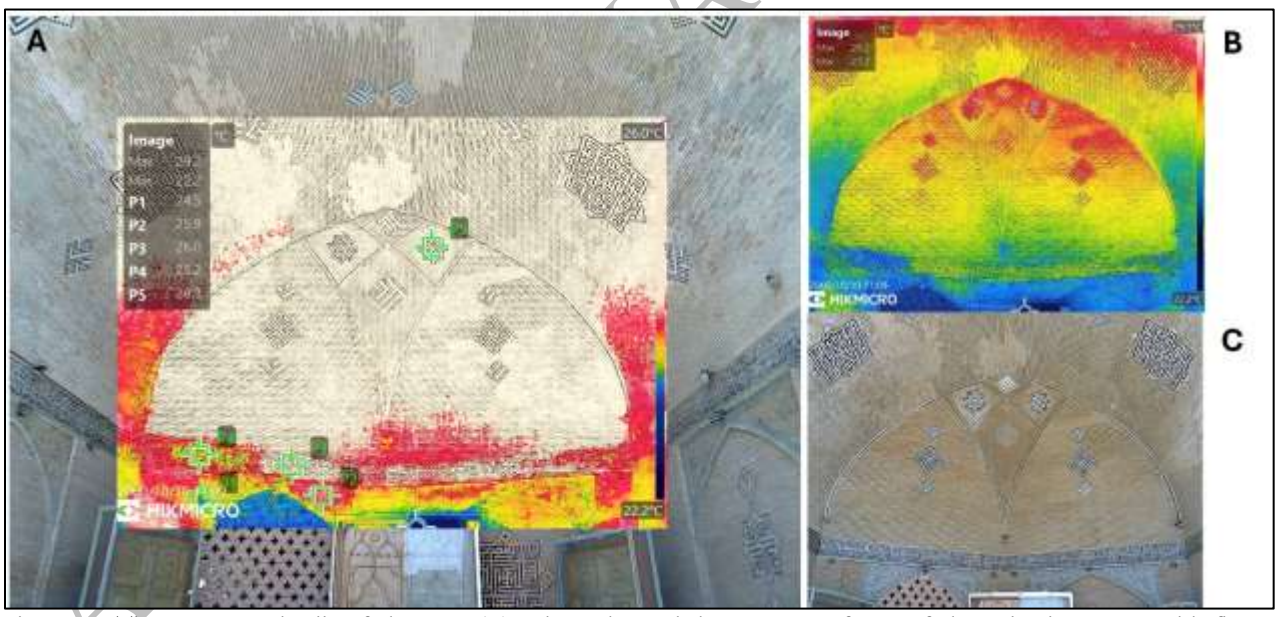



Figure 10. Thermograms details of the SM2 (A) Edge-enhanced thermogram of *ivan* of the Soltani Mosque, with five recorded measurement points (P1–P5). (B) thermogram with a recorded temperature range of 22.2–29.2°C (C) visible-light image of MS2;

Such thermal irregularities may indicate unstable conditions behind the tiled layers, potentially increasing the risk of more severe deterioration over time. Temperature differences in these areas may be associated with moisture accumulation, weakening of bonding mortars, and the initiation of layer detachment processes, particularly in locations with greater air exchange and more pronounced

ACCEPTED MANUSCRIPT

thermal fluctuations. Therefore, these areas can be identified as sensitive zones from a conservation perspective and require more detailed monitoring and complementary investigation using other non-destructive testing methods.

**4. Conclusions and future work**

This study demonstrates that infrared thermal imaging (IRT) is a highly effective, non-destructive, non contact tool for pre-screening of the conservation condition of historical tileworks and associated architectural materials. A key strength of the proposed approach is its speed: passive IRT allowed large façade areas to be screened in situ within a short time and pinpointed the zones at risk of deterioration, making it an efficient first step in a multi-stage diagnostic workflow.

Across the surveyed sites, IRT consistently revealed thermal contrasts between glazed tiles, stone, brick, and wood, providing clear evidence of each material's thermal behaviour and its implications for long-term structural performance. Stone, exhibited the greatest capacity for heat absorption and retention, promoting pronounced thermal gradients and internal stresses that can accelerate weathering over time. Temperature differentials between glazed tiles and surrounding masonry generated localized thermal gradients at material interfaces, an effect of particular concern where dissimilar materials are directly combined.

Most notably, these findings directly support the value of IRT as an early-warning tool for tile detachment. Precisely, the lower heat absorption may flags anomalies which may suggest degradation of the mortar behind the tile and its detachment. The greater heat absorption and retention observed in glazed tiles relative to surrounding bricks indicates an elevated long-term risk of delamination, and detachment. The survey identified stress concentration at the tile–mortar interface as a key precursor to reduced adhesion and moisture penetration—precisely the deterioration mechanism IRT is well suited to detect before it becomes visually apparent or structurally critical. Thermal anomalies documented across the muqarnas (SM1), tiled frames (GP2 and GP3), and stone surfaces consistently corresponded to areas of probable moisture accumulation or incipient delamination, confirming this diagnostic capability.

The integrated survey approach substantially improved understanding of the monumental complex's conservation state, and its short acquisition time and high analytical yield support its adoption within a broader preventive conservation protocol as a pre-screening approach. Together, these results establish infrared thermography as a reliable, efficient, and non-invasive diagnostic tool for the early detection and pre-screening of tile detachment, capable of meaningfully informing monitoring and conservation strategies for historic buildings.

**Limitations and Future Work**

As a passive, in situ screening approach, this study was carried out under natural environmental conditions. Solar exposure, shading and wind could therefore not be fully controlled, and evaluating anomalies as relative contrasts against same-material reference areas proved an effective way to account for this. The anomalies identified, including those potentially related to moisture, detachment and past restoration, provide a well-defined basis for targeted follow-up investigations. Future work could verify selected anomalies with techniques matched to each deterioration mechanism. Glaze detachment could be investigated with microscopic, spectroscopic methods, such as SEM, Raman, FTIR, XRF and multi and hyperspectral imaging, which characterise the glaze together with associated alteration products, salts and restoration materials. Tile detachment from ground could be investigated with radar, ultrasonic and hammer testing, which detect voids and loss

ACCEPTED MANUSCRIPT

of adhesion between the tile and its substrate. Repeated surveys across seasons, including freeze–thaw periods and full diurnal cycles, would further characterise the thermal behaviour of the tilework. Combining these approaches with active thermography on small test areas, heat-transfer modelling and multivariate analysis of thermal image sequences would help develop a robust, objective scheme for prioritising conservation interventions in Qajar tiled façades.

**Acknowledgements:** The author would like to express sincere gratitude to Eng. Mohammad Hasan Mohebbali for his technical assistance throughout this study and to Eng. Amin Mohebbali for his technical support and valuable collaboration during the IRT data acquisition process.

**Author Contributions:** The author was solely responsible for all aspects of this work, including conceptualization, methodology, data acquisition, analysis, and writing of the manuscript.

**Conflicts of Interest:** The author declares no conflict of interest.

**Funding:** This research received no external funding.

**Data Availability Statement:** The data supporting the findings of this study are available from the author upon reasonable request.

**References**

Allardice, B. (2012). https://www.flickr.com/photos/gballardice/7571636374

Barbosa, M. T. G., Rosse, V. J., & Laurindo, N. G. (2021). Thermography evaluation strategy proposal due moisture damage on building facades. Journal of Building Engineering, 43, Article 102555. https://doi.org/10.1016/j.jobe.2021.102555

Bashevskaya, O. S., Bushuev, S. V., Poduraev, Y. V., Mel'nichenko, E. A., Shcherbakov, M. I., & Garskov, R. V. (2017). Use of infrared thermography for evaluating linear dimensions of subsurface defects. Measurement Techniques, 60(5), 495–500. https://doi.org/10.1007/s11018-017-1217-0

Bomberg, M., & Shirtliffe, C. J. (1978). Influence of moisture and moisture gradients on heat transfer through porous building materials. In R. P. Tye (Ed.), Thermal transmission measurements of insulation (ASTM STP 660, pp. 211–233). American Society for Testing and Materials.

Çengel, Y. A., & Ghajar, A. J. (2015). Heat and mass transfer: Fundamentals and applications (5th ed.). McGraw-Hill Education.

Costanzo, A., Minasi, M., Casula, G., Musacchio, M., & Buongiorno, M. F. (2015). Combined use of terrestrial laser scanning and IR thermography applied to a historical building. Sensors, 15(1), 194–213. https://doi.org/10.3390/s150100194

de Melo, S. B., da Paz, R. F., & Mesquita, E. (2024). Recent advances on infrared thermography for ceramic tiles detachments diagnosis: Literature review. Journal of Building Rehabilitation, 9, Article 35. https://doi.org/10.1007/s41024-024-00387-6

Dritsa, V., Orazi, N., Yao, Y., Paoloni, S., Koui, M., & Sfarra, S. (2022). Thermographic imaging in cultural heritage: A short review. Sensors, 22(23), Article 9076. https://doi.org/10.3390/s22239076

ACCEPTED MANUSCRIPT

Fitzner, B., Heinrichs, K., & La Bouchardiere, D. (2002). Damage index for stone monuments. International Journal of Rock Mechanics and Mining Sciences, 39(3), 397–417. https://doi.org/10.1016/S1365-1609(02)00006-9

Ftikou, E. (2016). Criteria for the selection of materials and techniques for the conservation of historic mosaics substrate [Doctoral dissertation, National Technical University of Athens].

Gade, R., & Moeslund, T. B. (2014). Thermal cameras and applications: A survey. Machine Vision and Applications, 25(1), 245–262. https://doi.org/10.1007/s00138-013-0570-5

Grinzato, E., Bison, P. G., & Marinetti, S. (2002). Monitoring of ancient buildings by the thermal method. Journal of Cultural Heritage, 3(1), 21–29. https://doi.org/10.1016/S1296-2074(02)01159-7

Hall, C., & Hoff, W. D. (2011). Water transport in brick, stone and concrete (2nd ed.). CRC Press. https://doi.org/10.1201/b10911

Incropera, F. P., DeWitt, D. P., Bergman, T. L., & Lavine, A. S. (2011). Fundamentals of heat and mass transfer (7th ed.). Wiley.

Lawrence, M., & Walker, P. (2006). The thermal performance of traditional brick masonry. Construction and Building Materials, 20(10), 785–794. https://doi.org/10.1016/j.conbuildmat.2005.01.018

Ljungberg, S. A. (1994). Infrared techniques in buildings and structures: Operation and maintenance. In X. Maldague (Ed.), Infrared methodology and technology (Non-destructive Testing Monographs and Tracts, Vol. 7, pp. 211–252). Gordon & Breach Science Publishers.

Meola, C., Di Maio, R., Roberti, N., & Carlomagno, G. M. (2005). Application of infrared thermography and geophysical methods for defect detection in architectural structures. Engineering Failure Analysis, 12(6), 875–892. https://doi.org/10.1016/j.engfailanal.2004.12.030

Mercuri, F., Paoloni, S., Cicero, C., Zammit, U., & Orazi, N. (2018). Infrared emission contrast for the visualization of subsurface graphical features in artworks. Infrared Physics & Technology, 89, 223–230. https://doi.org/10.1016/j.infrared.2018.01.010

Moropoulou, A., Avdelidis, N. P., Delegou, E. T., Aggelakopoulou, M., Karoglou, G., Haralampopoulos, S., Griniezakis, M., Koui, P., Karmis, A., & Aggelopoulos, A. (2000). Investigation for the compatibility of conservation interventions on Hagia Sophia mosaics using NDT techniques. Journal of the European Study Group on Physical, Chemical, Biological and Mathematical Techniques Applied to Archaeology, 59, 103–120.

Neville, A. M. (2012). Properties of concrete (5th ed.). Pearson Education.

Orazi, N. (2020). Mid-wave infrared reflectography and thermography for the study of ancient books: A review. Studies in Conservation, 65(8), 437–449. https://doi.org/10.1080/00393630.2019.1706916

Paoloni, S., Mercuri, F., Orazi, N., Caruso, G., & Zammit, U. (2020). Photothermal approach for cultural heritage research. Journal of Applied Physics, 128(18), Article 180904. https://doi.org/10.1063/5.0023432

Sfarra, S., Fernandes, H. C., López, F., Ibarra-Castanedo, C., Zhang, H., & Maldague, X. (2018a). Qualitative assessments via infrared vision of sub-surface defects present beneath decorative surface coatings. International Journal of Thermophysics, 39, Article 13. https://doi.org/10.1007/s10765-017-2333-4

Sfarra, S., Regi, M., Tortora, M., Casieri, C., Perilli, S., & Paoletti, D. (2018b). A multi-technique nondestructive approach for characterizing the state of conservation of ancient bookbindings.

ACCEPTED MANUSCRIPT

Journal of Thermal Analysis and Calorimetry, 132, 1367–1387.https://doi.org/10.1007/s10973-018-6997-z

Steinhagen, H. P., & Haslett, A. N. (1993). Thermal properties of wood. Wood and Fiber Science, 25(4), 383–395.

Theodorakeas, P., Cheilakou, E., Ftikou, E., & Koui, M. (2015). Passive and active infrared thermography: An overview of applications for the inspection of mosaic structures. Journal of Physics: Conference Series, 655, Article 012061. https://doi.org/10.1088/1742-6596/655/1/012061

Theodorakeas, P., Cheilakou, E., Ftikou, E., & Koui, M. (2018). Long-term and sustainable approach to preserve ancient mosaic heritage: The case study of mosaic pavement located at the "Sanctuary of Pan," Pnyka (Athens). In M. Koui, F. Zezza, & D. Kouis (Eds.), Proceedings of the 10th International Symposium on the Conservation of Monuments in the Mediterranean Basin, MONUBASIN 2017 (pp. 105–113). Springer.

Tortora, M., Sfarra, S., Chiarini, M., Daniele, V., Taglieri, G., & Cerichelli, G. (2016). Non-destructive and micro-invasive testing techniques for characterizing materials, structures and restoration problems in mural paintings. Applied Surface Science, 387, 971–985. https://www.sciencedirect.com/science/article/abs/pii/S0169433216314507

Tortora, M., Sfarra, S., & Casieri, C. (2019). NMR relaxometry and IR thermography to study ancient cotton paper bookbinding. Applied Sciences, 9(16), Article 3406.https://doi.org/10.3390/app9163406

UNESCO. (2013). Golestan Palace. UNESCO World Heritage Centre.https://whc.unesco.org/en/list/1422/

Vavilov, V., Kauppinen, T., & Grinzato, E. (1997). Thermal characterization of defects in building envelopes using long square pulse and slow thermal wave techniques. Research in Nondestructive Evaluation, 9(4), 181–200. https://doi.org/10.1080/09349849709414473

Yang, X., Chen, B., Hu, G., Wang, X., Fang, W., Zhang, J., Tao, N., & Yuan, G. (2022). Pulsed infrared thermographic study of a Chinese Bronze Lei. Heritage Science, 10, Article 152. https://doi.org/10.1186/s40494-022-00791-6

Zandieh, M., Fahimi Far, A., Khaleghi, I., & Mohammadi Haji Abadi, F. (2013). The identity of the early Qajarid architectural decoration and its sources from the beginning to the end of Fat'h Ali Shah period (1785–1834). International Journal of Architectural Engineering & Urban Planning, 23(1–2).

ACCEPTED MANUSCRIPT